Electronic Supplementary Information

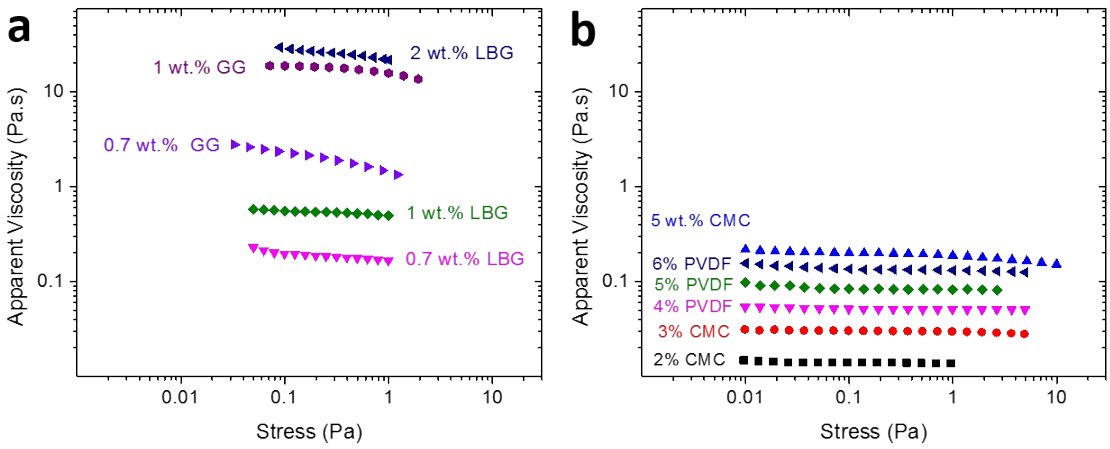

Figure S1. Steady-shear rheology of (a) galactomannan and (b) CMC and PVDF solutions; the concentration of each solution is labeled on the plots. As evident from comparison of the two graphs, galactomannans have a much higher viscosity than PVDF and CMC solutions.

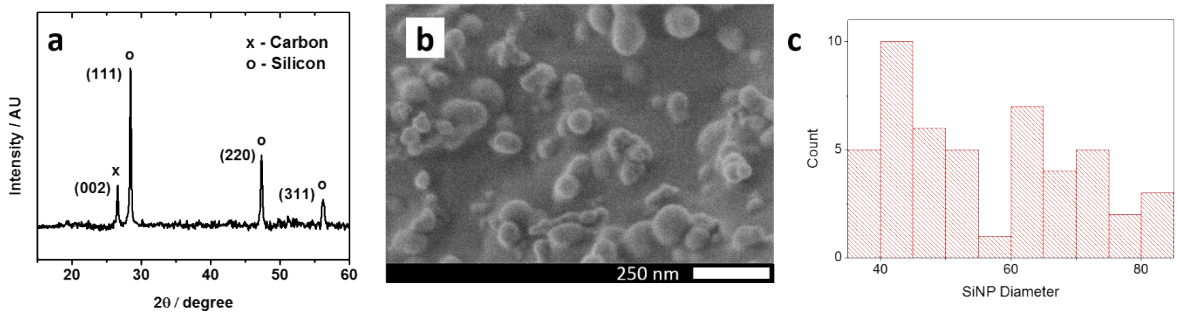

Figure S2. (a) XRD spectrum of the SiNP/GG electrodes used to determine the crystallite size of the SiNPs; (b) SEM image of the SiNPs on carbon tape and (c) the corresponding size distribution of the SiNPs as measured by HR-SEM images with average bi-modal particle size of 58 nm.

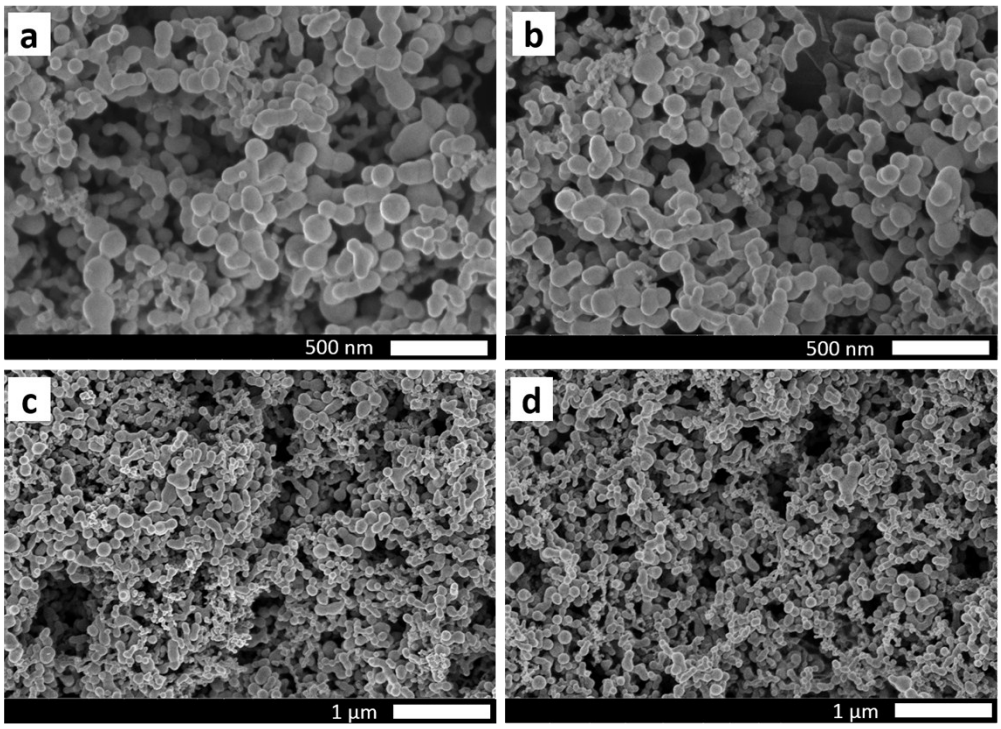

Figure S3. SEM images of SiNP/GG electrodes with (a) 10 wt% binder and (b) 15 wt% binder. As the concentration of binder increases, no dramatic decrease in film porosity is observed. Additionally, the size of the SiNPs encapsulated in the binder does not appear to increase as the binder loading increases. The same effect can be seen when the LBG concentration in the electrode increases from (c) 5 wt% to (d) 15 wt%.

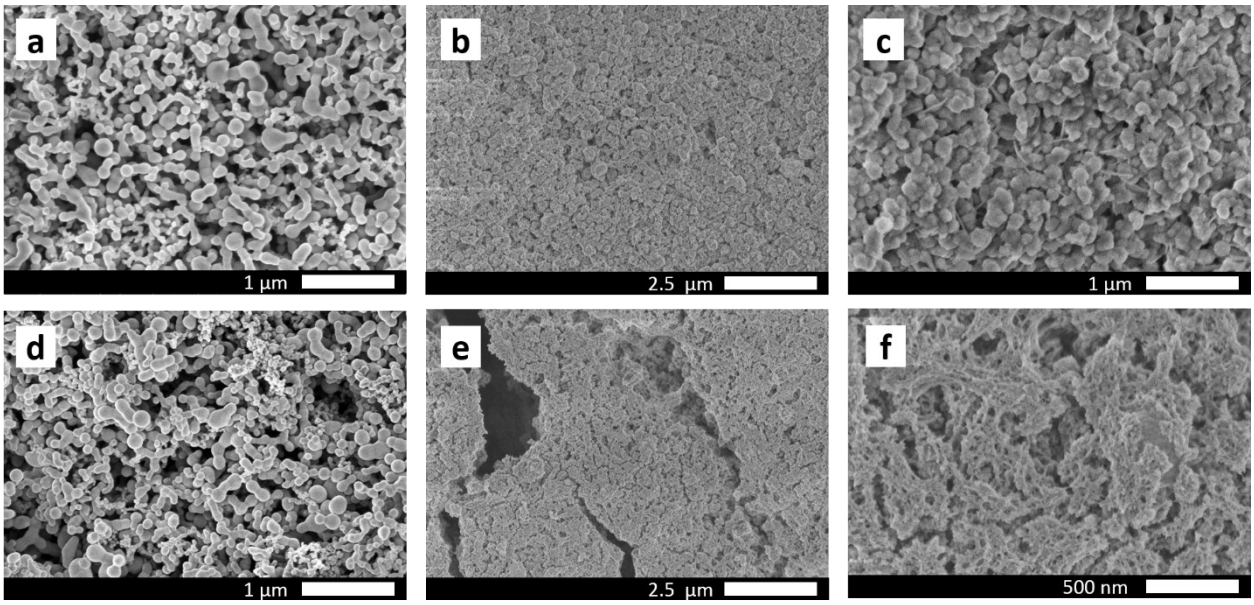

Figure S4. SEM images of pre-cycled (a) SiNP/PVDF and (d) SiNP/CMC electrodes. SiNP/PVDF electrodes appear to lose porosity and fuse together (b,c) upon cycling. A similar loss in pre-cycled electrode structure is observed in SiNP/CMC electrodes (e, f). Post-mortem images were captured after 50 charge/discharge cycles at 3.6 A g^{-1}.

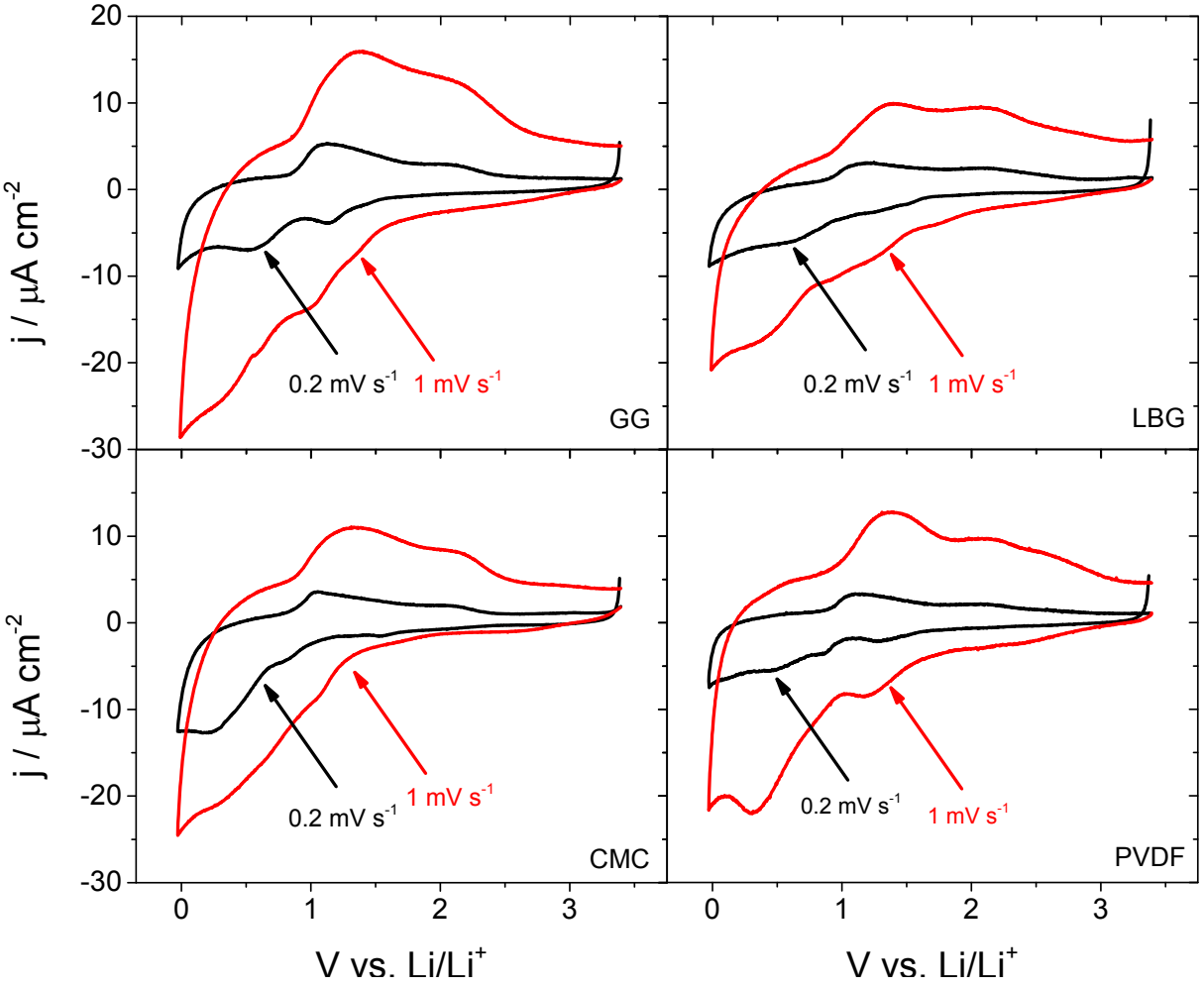

Figure S5. Cyclic voltammograms of (a) GG, (b) LBG, (c) CMC, and (d) PVDF polymer-only films on Cu foil indicate little current is produced with the binder materials. Additionally, given their electrochemical stability at potentials higher than 2 V vs Li/Li^+, GG and LBG may be candidates for alternative cathode binding materials.

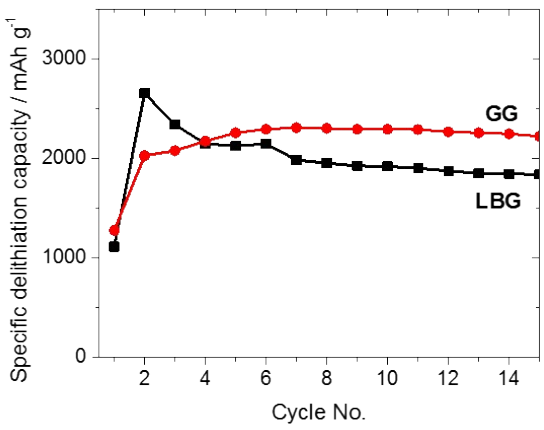

Figure S6. Cycling of SiNP electrodes in the absence of carbon with 100 mV cut-off voltage. The half-cells were lithiated to 1200 mAh g^{-1} at 0.1-C (360 mA g^{-1}) on the first cycle. On ensuing cycles the electrodes were lithiated under constant current to 100 mV at 0.1-C (360 mA g^{-1}) and held under constant voltage conditions until 0.01-C (36 mA g^{-1}). The binders allow for stable cycling at 0.1-C rates. The electrode contains 90 wt% SiNPs and 10 wt% binder.

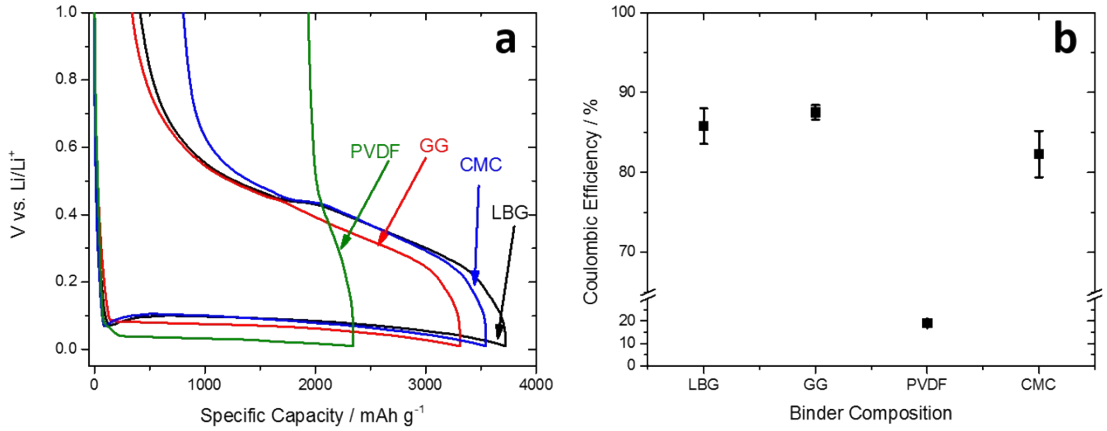

Figure S7. (a) Typical charge/discharge profiles of SiNP electrodes using various polymer binders. In the first lithiation the crystalline Si is converted to amorphous Si and the native-oxide layer is reduced to Si^0; (b) Average coulombic efficiencies of SiNP electrodes on the formation cycle. The galactomannan binders operate with the highest initial CEs. The electrodes composition is 85:10:5, SiNPs:C:Binder wt%.

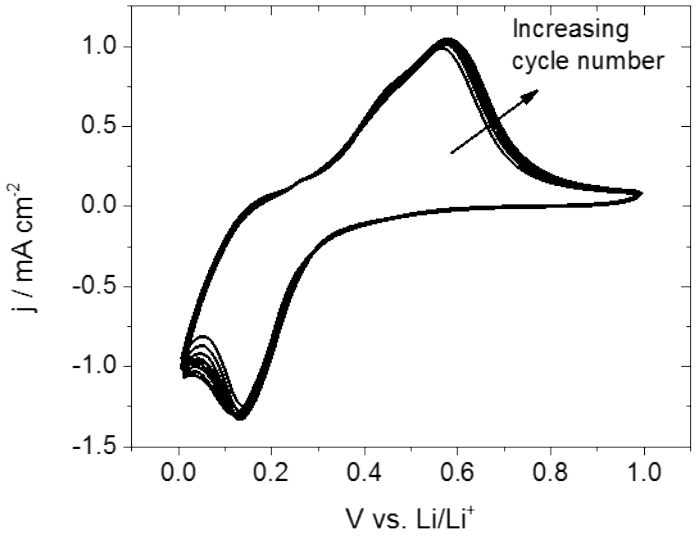

Figure S8. CV cycles 11-20 of a SiNP/LBG electrode. A maximum peak current density is attained after the 13th cycle. The half-cell was cycled between 1 V and 0.01 V vs Li/Li^+ using a scan rate of 0.2 mV s^{-1}. Electrode composition is 85:10:5, SiNPs:C:LBG wt%.

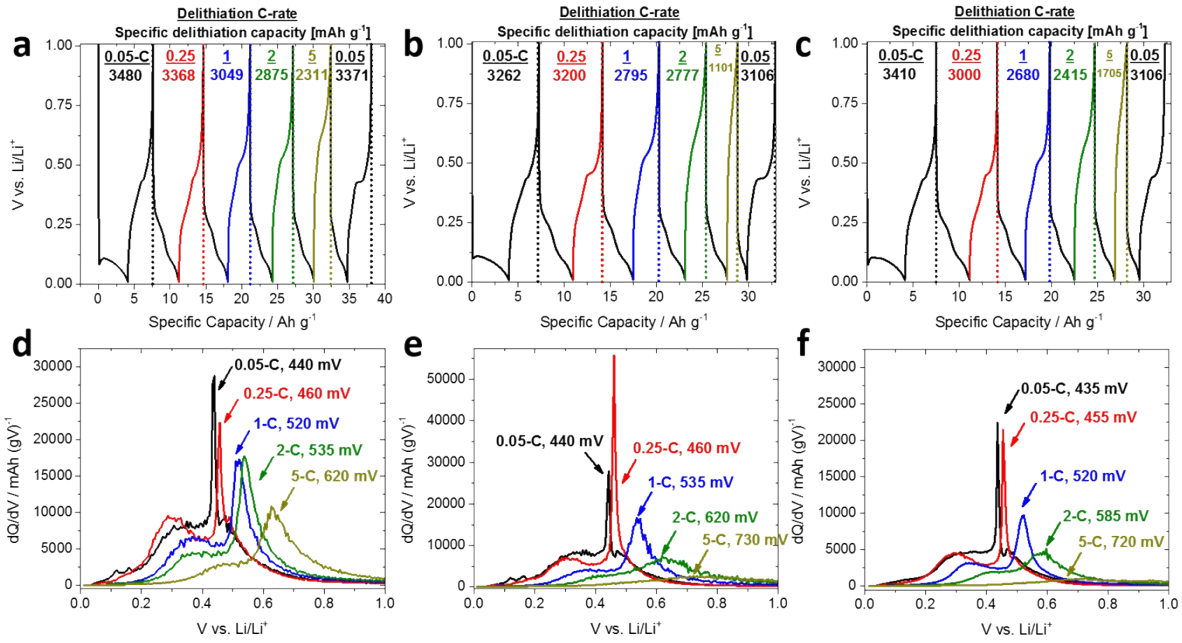

Figure S9. Asymmetric charge-discharge profile curves of SiNP electrodes using (a) GG (b) LBG and (c) CMC electrodes, as well as the corresponding differential capacities for the delithiation curve for the electrodes using (d) GG and (e) LBG and (f) CMC binders. All lithiation rates are 0.05-C to ensure full lithiation.

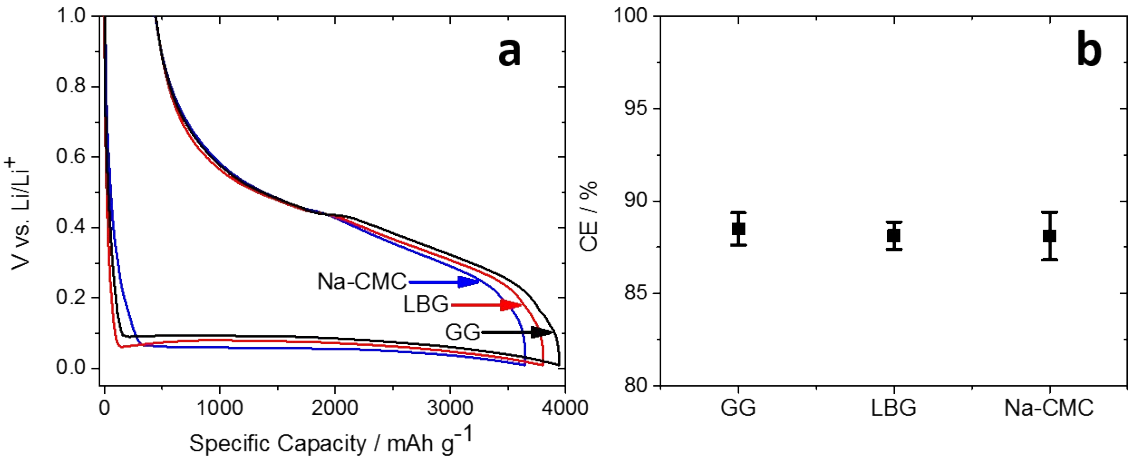

Figure S10. Typical (a) charge/discharge profiles of the formation cycle when binder loading is increased to 15 wt% and the (b) corresponding CEs reveal high CEs of ~88% (b). Electrode composition is 75:10:15, SiNPs:C:Binder wt%.

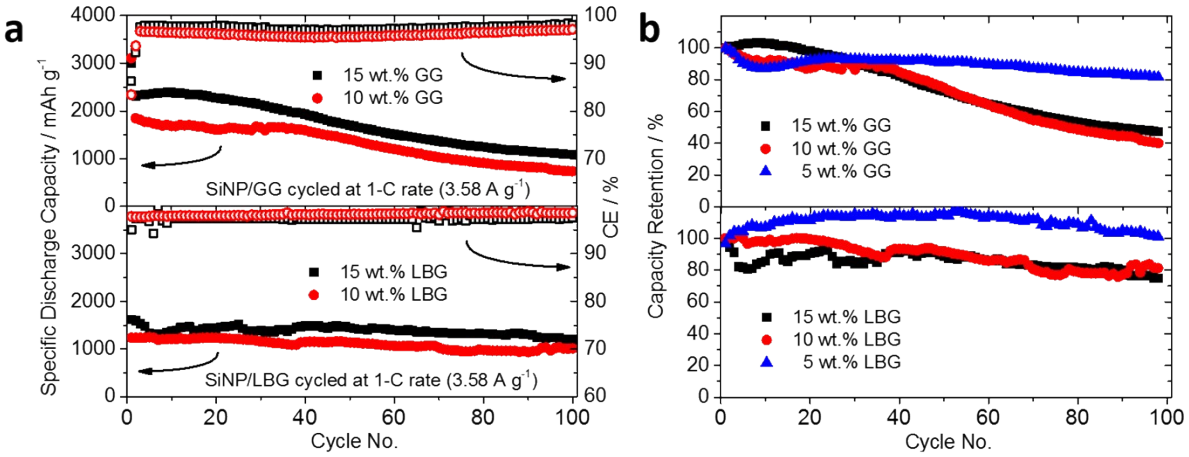

Figure S11. (a) Delithiation capacity and coulombic efficiency of SiNP electrodes using 10 and 15 wt% GG and LBG over 100 cycles at 1-C rate and (b) the capacity retention corresponding to (a). The capacity data from 5 wt% can be seen in Figure 7a in the text. As the amount of binder increases, so too does the irreverble capacity loss.